Bulletin of Electrical Engineering and Informatics
Vol. 12, No. 5, October 2023, pp. 2816~2823
ISSN: 2302-9285, DOI: 10.11591/eei.v12i5.5163

Improving the color deviation of white light emitting diode by employing $Sr_3Ga_2Ge_4O_{14}:Cr^{3+}$ phosphor

Ha Thanh Tung[1], Huu Phuc Dang[2], Dieu An Nguyen Thi[3]
[1]Faculty of Basic Sciences, Vinh Long University of Technology Education, Vinh Long Province, Vietnam
[2]Faculty of Fundamental Science, Industrial University of Ho Chi Minh City, Ho Chi Minh City, Vietnam
[3]Faculty of Electrical Engineering Technology, Industrial University of Ho Chi Minh City, Ho Chi Minh City, Vietnam

Article Info

Article history:

Received Nov 7, 2022
Revised Dec 16, 2022
Accepted Jan 11, 2023

Keywords:

Chromaticity
Color quality scale
Color rendering index
$Sr_3Ga_2Ge_4O_{14}:Cr^{3+}$
White light-emitting diode

ABSTRACT

The pomising uses of near infrared (NIR) phosphor converted light emitting diodes (pc-LEDs), including non-destructive testing and biological implementations, are endless. It is still difficult to create wideband and NIR phosphors with sufficient heating steadiness for a variety of uses. The study herein introduces the phosphor $Sr_3Ga_2Ge_4O_{14}:Cr^{3+}$, its creation procedure through expreiments as well as its influneces on LED devices. The $Sr_3Ga_2Ge_4O_{14}:Cr^{3+}$ (SGGO:Cr^{3+}) super-wideband NIR phosphor was effectively synthesized in this study with 431 nm stimulation, and a spectrum adjustment 750 nm-900 nm was made in a two-step super-wideband radiation having its full width under half maximum (FWHM) changing among 257 and 336 nm. The inner quantum performance (IQP) for SGGO:0.15Cr^{3+} is 36.67%, and it has an FWHM of 257 nm. At 423 K, the emitting strength was still 76% of ambient temperature. The potential of SGGO:Cr^{3+} for various uses was eventually demonstrated by the employment of SGGO:0.03Cr^{3+} as well as SGGO:0.15Cr^{3+} samples accompanied by blue illumination chips under 430 nm for the task of creating NIR pc-LED gadgets then putting in nighttime sight, human palm puncture, flora lighting. It was shown that SGGO:Cr^{3+} has a wide range of use possibilities.

Corresponding Author:

Huu Phuc Dang
Faculty of Fundamental Science, Industrial University of Ho Chi Minh City
No. 12 Nguyen Van Bao Street, Ho Chi Minh City, Vietnam
Email: danghuuphuc@iuh.edu.vn

1. INTRODUCTION

Owing to its outstanding qualities, including invisibility, elevated penetration, and non-invasive procedures [1], [2], near infrared (NIR) (700–1700 nm) illumination has received an excellent agreement of people's attention in the sectors of night sight lighting [3], [4], plant illumination [5], [6], biological photography, and non-destructive evaluating [6]–[9]. Despite achieving a wideband radiation from the visible to the NIR, classic NIR light supplies including light emitting diode (LED), halogen lights, along with very long-wavelength lasers still have a variety of drawbacks, including limited effectiveness, excessive size, and elevated functioning heats [7], [8]. The strait band of hues of NIR LEDs (full width under half maximum (FWHM) 50 nm) can be effective and energy-saving, but it is insufficient for the wideband illumination needed for detection. These problems can be rectified by NIR phosphor converted light emitting diodes pcLEDs, which are anticipated to be the future NIR illumination supplies because to their strong radiative intensity, cheap price, and straightforward production process [9], [10]. These LEDs comprise one blue

InGaN chip as well as wide-band NIR-discharging phosphor. As a result, the main focus of NIR phosphor converted light emitting diodes pc-LEDs is the quest for satisfactory NIR phosphors [11].

The rare-earth ions, including Nd^{3+}, Tm^{3+}, Pr^{3+}, as well as Yb^{3+}, would be predominantly f-f inhibited transformation radiation, faint absorptibity, strait FWHM, along with poor quantum effectiveness, which may not fulfill the realistic demands [12]. The other category of activation ions is transformation metal ions, including Mn^{2+} and Cr^{3+}. Whereas Cr^{3+} ions' d-d transformation typically illustrates wideband absorbance and radiation in contrast to the f-f inhibited transformation for rare-earth ions, with the emitting range being nearer towards the directional long-wave than Mn^{2+}-doped substances as well, their emitting band of hues are primarily within the directional short-wave inside the intense red NIR range, making them inferior when it comes to food identification and biological puncturing. Consequently, it is a pressing issue to build wideband generating NIR phosphor with excellent heating steadiness and quantum effectiveness [13], [14].

The choice of an appropriate host will significantly improve the efficiency of the substance because the phosphor base as well as triggering ion are the main variables determining substances' luminous qualities. According to the publications that have already been published and the investigation of the Cr^{3+} illumination process, it is recommended that hosts with numerous crystallographic lattices be used like stuffs to enable multi-lattice Cr^{3+} radiation and a broader bands of colors. Our study curiosity was piqued by Tsai *et al*. [15] proposal of a super-wideband NIR sample having an FWHM reaching 330 nm, $La_3Ga_5GeO_{14}:Cr^{3+}$ in 2018. For its chaotic (or statistical) dispersion within the multi-sheet crystal configuration, the Ca-gallogermanate family (space group P321) can create several sites appropriate for Cr^{3+} doping. Through controlling the dosage of Cr^{3+}, the spectra were also changed from 900 to 750 nm, and the FWHM was consistently kept among 257 and 336 nm. With the use of an NIR camera, studies on plant development lighting, night vision lighting, and human blood vessel imaging, it has been demonstrated that SGGO:Cr^{3+} would be a potential multi-purpose NIR sample.

2. EXPERIMENTAL

2.1. Synthesis

The elevated-heat solid phase response technique was used to successfully make $Sr_3Ga_2Ge_4O_{14}:xCr^{3+}$ ($0 \leq x \leq 0.20$) phosphors. The initial components $SrCO_3$, Ga_2O_3 (99.99%), GeO_2 (99.9999%), and Cr_2O_3 were weighed and ground for 30 minutes in an agate mortar according to the intended mixture. The combination was then transferred to one corundum crucible then put inside a muffle furnace. In there, the blend underwent sintering for 6 hours under 1,250 °C. The furnace was then allowed to cool naturally to ambient heat, and the specimens were crushed into a fine powder for further analysis [16].

2.2. Characterization

Using an X-ray diffractometer and Kα radioactivity for one Cu subject bypassing Ni lines (λ=0.15405 nm), the purity of the phases was determined. The diffraction range and step size are 0.02° and 10-80°, respectively, while the functioning parameters reach 40 milliamperes as well as 40 kilovolts. Using the GSAS tool, Rietveld rectification was done within the 10-80° scope. EDS and area emitting scanning electron microscopy were utilized to assess the morphology and content of the samples [17]. Via a 450-W Xe light serving in the form of the stimulation mean under 1500 V, the emitting band of colors and stimulation band of colors at normal heat were evaluated on a fluorescence spectrophotometer, and the changeable heating band of colors (between 298 K and 473 K) as well as the life degradation arch under poor heat (4 K) were evaluated via outer heat managing gadgets. With $BaSO_4$ serving like the test background, dispersed reflection bands of colors in the 240-900 nm region were recorded.

2.3. Manufacture of NIR pc-LED gadgets

One InGaN chip under 430 nm combined with SGGO:Cr^{3+} makes up the NIR pc-LED element. The silica gel should be mixed well with the correct quantity of phosphors for 20 minutes. The resultant slurry was applied to said chips' exterior then let dry under 80 ^oC to create NIR pc-LED gadgets. The best generating gadget was chosen and powered at 5-105 mA current under a 30 mA current drive. Figure 1 displays the technical details of white light emitting diodes (WLEDs) [17]. The WLED device employed for the study herein can be seen Figure 1(a). Figures 1(b)-(d) show the binding graph, graphical illustration of WLED, and WLED recreation through the LightTools program.

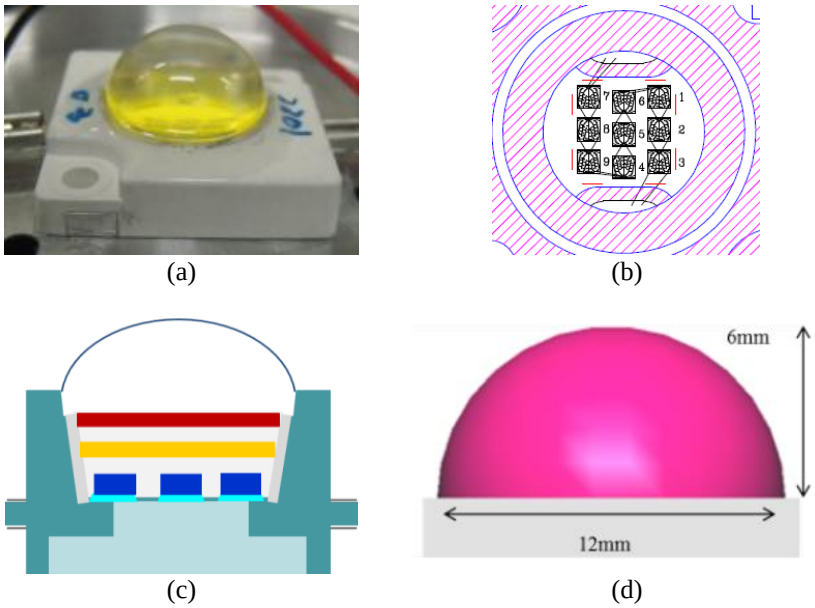

Figure 1. Picture concerning WLED formation (a) WLED device used for study, (b) binding graph, (c) pc-WLEDs illustrated, (d) WLED recreation utilizing LightTools program

3. RESULTS AND DISCUSSION

In order to create an illumination supply with great effectiveness and respectable emitting hue properties, the right mixture containing proficient phosphor samples would be obviously important. The phosphors ability to be excited, or the extent in which their stimulating bands of colors correspond to the pumping LED discharge, would be a second crucial factor in determining the effectiveness of phosphors. In fact, this is the primary cause of the perfectly tuned fluorescent lamp phosphors' mostly ineffective usage in LED applications. The mercury emission line at 254 nm mostly stimulates these phosphors. We need to avoid producing pumping LED devices having radioactivity within such a wavelength scope for reasons of energy effectiveness. As such, it is necessary to choose phosphors with excellent excitability in the close-UV to blue area of the spectrum. Moreover, the stimulating spectrum needs to be extensive enough for the task of making up for disparities within the pumping LED's discharging band for colors brought on by changings in the conducting current and/or joint heat. As such, we would need a somewhat flat stimulating spectrum in the phosphors roundly the peak emission of the LED in order to maintain hue boost pumping LEDs having radioactivity within said wavelength scope stability over the whole wLED. It makes sense to use the wide band releasing rare earth ions (Eu^{2+} along with Ce^{3+}), since their stimulation spectra also contains a number of rather wide bands [18], [19].

The heat behavior of the conversion phosphor is crucial when it is placed close to the LED chip. In fact, with one proficient LED with an input power reaching 5W and a total effectiveness of 150 lm/W, only 3 W of heat must be dispersed by the gadget while nearly 40% of the input power gets transformed into optic energy. The phosphor’s Stokes losses, non-radioactive degradation, as well as non-radioactive remixing within the pumping LED are clearly connected to the losses. In the manufacturing of an LED, heat management is a crucial consideration because of the tiny chip surface and the constrained phosphor area. However, temperatures between 400 and 450 K may be attained close to the LED chip. As a result, even at these high heats, the phosphor ought to retain its quantum effectiveness and spectrum properties. The radiation and stimulation spectra should ideally match as a function of temperature. The occupancy of higher vibrational levels causes the emitting spectra of Eu^{2+} and Ce^{3+} to widen with temperature. It's also conceivable for the peak emitting position to vary. For the rare earth that emits 4f-4f.

When developing LEDs, one should pay same notice to the effectiveness of the complete converting procedure from electrical power to the observable optic power in addition to the form of the emitting spectrum. Utilizing phosphors with quantum effectiveness near to agreement is crucial to achieving such a high effectiveness. If an exact assessment of the quantum effectiveness is not feasible, one should at the very least contrast it with a recognized converting phosphor that exhibits comparable stimulation behavior. It goes without saying that when comparing emissions, integrated emission strengths rather than peak emission strengths should be used. This is particularly valid when contrasting strait-band emitters with line emitters.

The word "quantum efficiency" was utilized to characterize the inner quality of the luminescence converting process known as the inner quantum performance (IQP), or the scale among the photons' quantity released and the photons' quantity subjected to absorption. The external quantum effectiveness should also be taken into consideration when evaluating a particular phosphor when it is used in an LED gadget. This is the product of the IQP times the proportion of the stimulation illumination that was absorbed or, alternatively, the scale of the photons' quantity released to the amount of photons incident. In general, the absorption at the stimulation wavelength raises as the dopant dosage in a phosphor rises. The trade-off among rising absorption (and emission) and falling internal quantum effectiveness as a result of dosage quenching, however, occurs. When used in LED applications, phosphors with high external quantum efficiencies enable the usage of little phosphor substance on the LED chip. This reduces the down-transformed light's absorption losses. As opposed to saying, band-discharging rare earth ions yielding weak absorptivities in the case of the 4f-4f changings, we should employ doping ions yielding elevated absorption cross sections.

Although the majority of proficient converting phosphors are depending on (wide range releasing) rare earth ions, it has also been reported that transition elements (including Mn^{2+} and Cr^{3+}) along with s^2 ions (Pb^{2+}, Bi^{3+}, $Sb^{3+,}$) are also used as dopants. In order to increase light production in the (intense) red region of the spectrum, some publications describe using phosphors that have been doped with Cr^{3+}. Strong Cr^{3+} emission with a 700 nm center could be produced when YAG:Ce^{3+} was co-doped; this emission was made stronger by power transition from the Ce^{3+} ions. As our sight responsiveness is extremely weak under such wavelengths, the pragmatic application for Cr^{3+} in WLED apparatuses, however, would be quite constrained. The cubic exponential function may be used to explain the SGGO degradation curve [20]:

$$I_t = I_0 + A_1\, exp\left(\frac{-t}{\tau_1}\right) + A_2\, exp\left(\frac{-t}{\tau_2}\right) + A_3\, exp\left(\frac{-t}{\tau_3}\right) \quad (1)$$

where I_t is the luminance, I_0 is the beginning luminance, A_1, A_2, and A_3 signify the fitting constants, τ is the duration, τ_1, τ_2, and τ_3 signify the exponential element's degradation times, and the median life τ^* is calculated using the method in (2) [21]:

$$\tau * = \frac{A_1\tau_1^2 + A_2\tau_2^2 + A_3\tau_3^2}{A_1\tau_1 + A_2\tau_2 + A_3\tau_3} \quad (2)$$

The highest points in the stimulation band of colors and the DRS exhibit excellent agreement. The Kubelka-Munk function can be used to determine the specimens' optic bandgap in the manner described in (3) and (4) [22]:

$$F(R) = \frac{(1-R)^2}{2R} \quad (3)$$

$$\alpha hv = c\left(hv - E_g\right)^{\frac{1}{2}} \quad (4)$$

The host lattice's crystal field environment has a significant impact on the generation of Cr^{3+} ions. It makes sense to determine the crystal area strengths independently when the PL bands of colors are a mixture of the bands of colors created when Cr^{3+} enters various lattices [23], [24].

$$10 \cdot D_q = E\left({}^4T_2\right) = E\left({}^2A_2 \rightarrow {}^4T_2\right) - \Delta S/2 \quad (5)$$

$$\frac{D_q}{B} = \frac{15\cdot(\Delta E/D_q - 8)}{(\Delta E/D_q)^2 - 10(\Delta E/D_q)} \quad (6)$$

$$\Delta E = E\left({}^4T_1\right) - E\left({}^4T_2\right) = E\left({}^4A_2 \rightarrow {}^4T_1\right) - E\left({}^4A_2 \rightarrow {}^4T_2\right) \quad (7)$$

where the Racah parameter B denotes the interaction among electrons within the third-order orbitals, and D_q signifies the crystal field splitting power strongly connected to the metal-ligand gap. The maxima in the disperse absorption ranges represent the equilibrium locations E($^4T_1$), and E($^4T_2$) of the $^4T_1$ and $^4T_2$ energy levels, respectively. The Stokes shift is ΔS. Due to (5)-(7), D_q/B was determined to be 2.11, 1.87, and 1.75 at 750, 900, and 1000 nm, correspondingly, demonstrating that Cr^{3+} is emitting wideband light when in a weak field condition.

Figure 2 exhibited the scattering coefficients (Sc) of the light emission with the increase in SGGO:Cr^{3+} phosphor concentration. The concentration increase of SGGO:Cr^{3+} phosphor stimulates the Sc, allowing more scattering of blue-chip emitted light to be transmitted and converted to greater-wavelength

lights. Such phenomenon can increase the luminescence if the amount of blue light scattered in the forward emission increase while blue-light reabsorption and backscattering are reduced. To serve this objective, the YGA:Ce yellow phosphor's concentration need to be lower when the SGGO:Cr^{3+} concentration become higher. This moreover helps to reduce the fluctuation of the correlated color temperature (CCT). The decreased YGA:Ce concentration with increasing SGGO:Cr^{3+} concentration was presented clearly in Figure 3, while the stability of CCT at higher concentration can be seen in Figures 4 and 5. Furthermore, in Figure 4, the ability to reduce the CCT variation (D-CCT) of the phosphor at higher doping concentration was obviously depicted. Though the D-CCT presented a clear fluctuation, it eventually bottoms out at around 70 K with 30% SGGO:Cr^{3+}, reduced by 100 K compared to the value when no SGGO:Cr^{3+} was used.

Figure 6 illustrates how the luminous strength of the white light emission was not always improved by the rise in SGGO:Cr^{3+} proportion. As shown, using 25% SGGO:Cr^{3+} produced the maximum luminosity, and using 30% SGGO:Cr^{3+} caused a noticeable luminous decline. It is also the maximum, with reference to the D-CCT value at 0% SGGO:Cr^{3+} in Figure 5. Due to higher back-scattering and reabsorption, this shows an unbalanced color distribution and decreased blue emission strength. As the phosphor absorbs more backscattered blue light, greater SGGO:Cr3+ dosages in particular would encourage the light conversion from blue to yellow or orange-red. As the phosphor layer tends to thicken with rising SGGO:Cr^{3+} quantity, the transformed illumination would then be reflected several times, degrading the total emission spectrum power. To put it another way, if the phosphor dosage is too high, more transformed illumination may be back-reflected, reducing luminous intensity while raising CCT. As a result, 25% of SGGO:Cr^{3+} was chosen as the appropriate amount for the simulated WLED in order to achieve improved color uniformity and luminous strength.

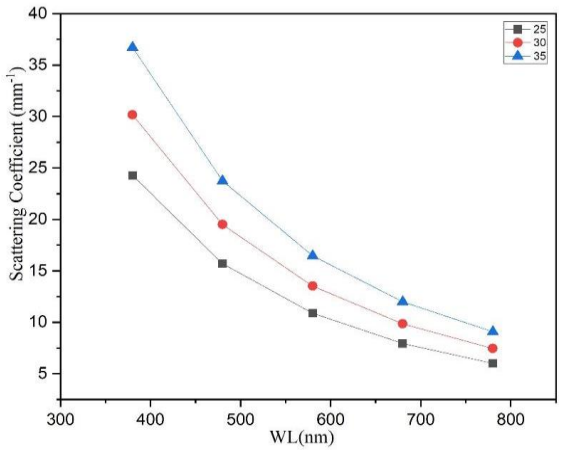

Figure 2. Scattering coefficients with various SGGO:Cr^{3+} phosphor dosages

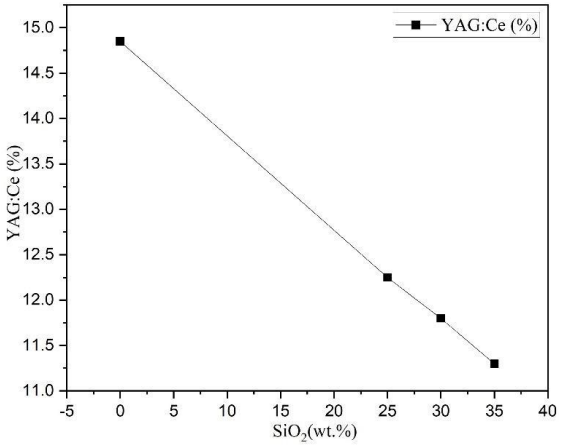

Figure 3. YGA:Ce phosphor dosage values with various SGGO:Cr^{3+} phosphor dosages

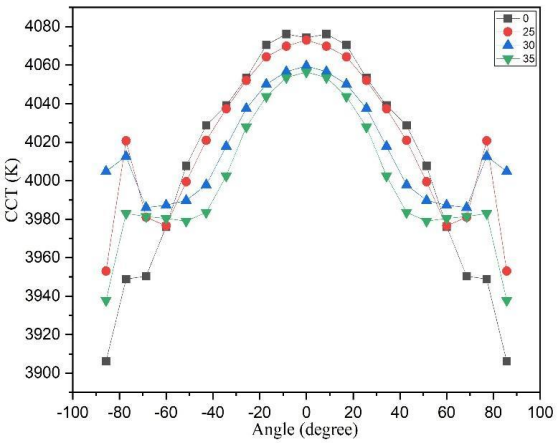

Figure 4. CCT values with various SGGO:Cr^{3+} phosphor dosages

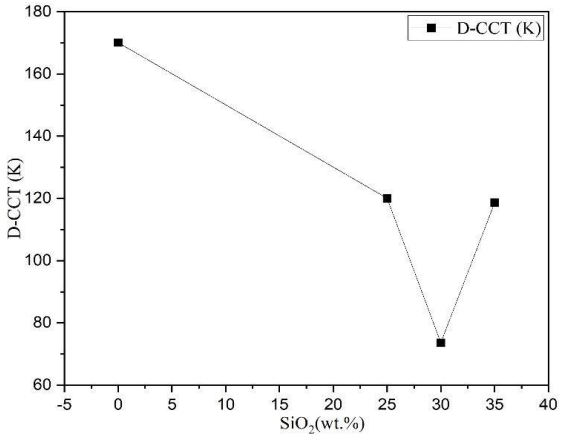

Figure 5. Color difference values with various SGGO:Cr^{3+} phosphor dosages

In addition to having an impact on brightness, the dosage of SGGO:Cr^{3+} phosphor has a significant impact on how well the white LED renders colors. As the concentration of SGGO:Cr^{3+} rises to 35% in Figures 7 and 8, color rendition values measured with the hue rendering indicator (CRI) and hue quality scale (CQS), showed a continual decline. Unbalanced blue, green, and yellow-orange patterns may be to blame for the significant decreases in CRI and CQS [25]. As was already indicated, as the light emission hue tends to lean more toward the yellow-orange area, there is an imbalance due to enhanced scattering from the high SGGO:Cr^{3+} dosage. As a result, the CRI and CQS will be reduced by excessive dispersion. This phosphor requires more research on other factors, such as the particle size, which will be examined in our research investigation, in order to manage the CRI and CQS.

Figure 9 showed the WLED's emitting spectra by utilizing SGGO:Cr^{3+} phosphor. The total white emitting band demonstrated that phosphor helps to increase the power of the blue and orange-red radiation. It is possible to alter the illumination efficiency by changing the SGGO:Cr^{3+} phosphor settings to affect the scattering and absorbing patterns of the WLED's light emission. The highest points may be seen in the blue (450 nm) and yellow-orange (~600 nm) areas.

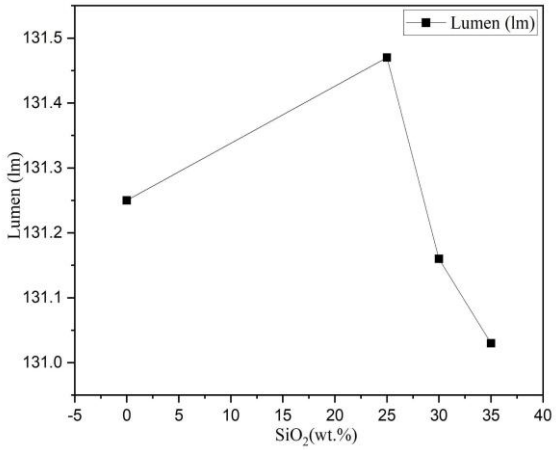

Figure 6. Luminescence strength with various SGGO:Cr^{3+} phosphor dosages

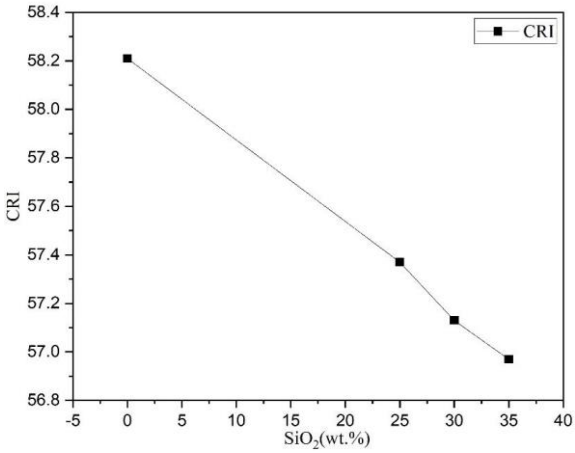

Figure 7. CRI values of the WLED with various SGGO:Cr^{3+} phosphor dosages

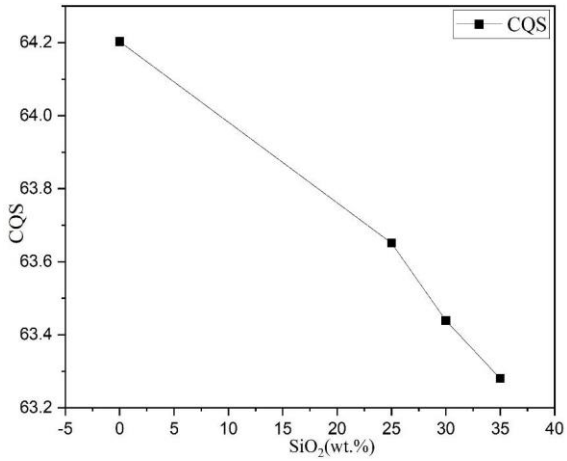

Figure 8. CQS values with various SGGO:Cr^{3+} phosphor dosages

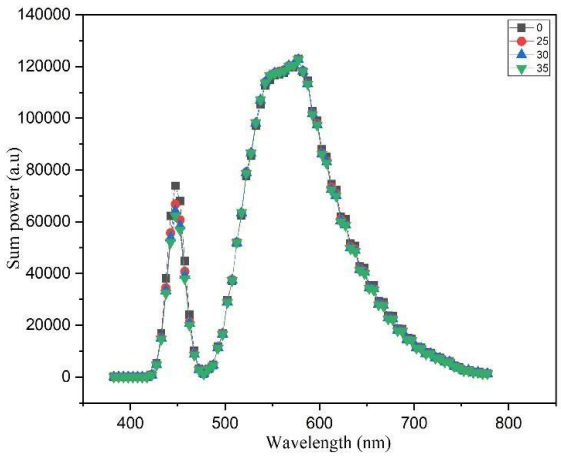

Figure 9. Luminescence power of the WLED with various SGGO:Cr^{3+} phosphor dosages

4. CONCLUSION

In conclusion, the effective synthesis of the super-wideband NIR phosphor Sr_3Ga_2-Ge_4O_{14}:-xCr^{3+}. Adjust able spectrum locations and strengths may be obtained by varying the dosage of Cr^{3+}, which results in the production of two phases of luminescence. With 431 nm stimulation, the SGGO:0.15Cr^{3+} phosphor

produces an asymmetric emitting band between 650 and 1300 nm with an FWHM of 257 nm. The SGGO:0.15Cr^{3+} has a 36.67% quantum effectiveness and a 76% heat steadiness, accordingly. Because of the dispersion for Ga/Ge ions from SGGO, Cr^{3+} settles in some positions, with low-temperature spectra and Raman spectra used to explain the occupancy of Cr^{3+} at various phases in detail. In order to show the possible uses of SGGO:Cr3+ in various domains, SGGO:0.03Cr^{3+} and SGGO:0.15Cr^{3+} were converted into NIR pc-LED device and used for night vision gadgets, human hand penetration investigations, and plant illumination, in turn. Therefore, by choosing substances with various crystal latticework positions appropriate in the case of Cr^{3+} replacement in the form of phosphor bases, our study demonstrates the viability of generating robust thermally steady wideband NIR phosphors.

REFERENCES

[1] H.-Y. Yu *et al.*, "Solar spectrum matching with white OLED and monochromatic LEDs," *Applied Optics*, vol. 57, no. 10, pp. 2659–2666, 2018, doi: 10.1364/AO.57.002659.

[2] Z. Zhao, H. Zhang, S. Liu, and X. Wang, "Effective freeform TIR lens designed for LEDs with high angular color uniformity," *Applied Optics*, vol. 57, no. 15, pp. 4216–4221, 2018, doi: 10.1364/AO.57.004216.

[3] J. O. Kim, H. S. Jo, and U. C. Ryu, "Improving CRI and scotopic-to-photopic ratio simultaneously by spectral combinations of cct-tunable led lighting composed of multi-chip leds," *Current Optics and Photonics*, vol. 4, no. 3, pp. 247–252, 2020, doi: 10.3807/COPP.2020.4.3.247.

[4] Y. Zhou *et al.*, "Comparison of nonlinear equalizers for high-speed visible light communication utilizing silicon substrate phosphorescent white LED," *Optics Express*, vol. 28, no. 2, pp. 2302–2316, 2020, doi: 10.1364/OE.383775.

[5] N. D. Q. Anh, P. X. Le, and H. Y. Lee, "Selection of a remote phosphor configuration to enhance the color quality of white LEDs," *Current Optics and Photonics*, vol. 3, no. 1, pp. 78–85, 2019, doi: 10.3807/COPP.2019.3.1.078.

[6] Y. Li, X. Zhang, H. Yang, X. Yi, J. Wang, and J. Li, "Effects of remote sediment phosphor plates on high power laser-based white light sources," *Optics Express*, vol. 29, no. 15, pp. 24552–24560, 2021, doi: 10.1364/OE.433581.

[7] S.-W. Jeon *et al.*, "Optical design of dental light using a remote phosphor light-emitting diode package for improving illumination uniformity," *Applied Optics*, vol. 57, no. 21, pp. 5998–6003, 2018, doi: 10.1364/AO.57.005998.

[8] Y. Fang *et al.*, "Giant enhancement of white light emission from Ca 9 Ln(PO 4) 7 :Eu 2+, Mn 2+ (Ln = La, Lu, Gd) phosphors achieved by remote aluminum reduction," *Optical Materials Express*, vol. 10, no. 5, pp. 1306–1322, 2020, doi: 10.1364/OME.390069.

[9] O. H. Kwon, J. S. Kim, J. W. Jang, and Y. S. Cho, "Simple prismatic patterning approach for nearly room-temperature processed planar remote phosphor layers for enhanced white luminescence efficiency," *Optical Materials Express*, vol. 8, no. 10, pp. 3230–3237, 2018, doi: 10.1364/OME.8.003230.

[10] Y. Tang, Z. Li, G. Liang, Z. Li, J. Li, and B. Yu, "Enhancement of luminous efficacy for LED lamps by introducing polyacrylonitrile electrospinning nanofiber film," *Optics Express*, vol. 26, no. 21, pp. 27716–27725, 2018, doi: 10.1364/OE.26.027716.

[11] Q. Guo *et al.*, "Characterization of YAG:Ce phosphor dosimeter by the co-precipitation method for radiotherapy," *Applied Optics*, vol. 60, no. 11, pp. 3044–3048, 2021, doi: 10.1364/AO.419800.

[12] H. Yuce, T. Guner, S. Balci, and M. M. Demir, "Phosphor-based white LED by various glassy particles: control over luminous efficiency," *Optics Letters*, vol. 44, no. 3, pp. 479–482, 2019, doi: 10.1364/OL.44.000479.

[13] L. Yang, Q. Zhang, F. Li, A. Xie, L. Mao, and J. Ma, "Thermally stable lead-free phosphor in glass enhancement performance of light emitting diodes application," *Applied Optics*, vol. 58, no. 15, pp. 4099–4104, 2019, doi: 10.1364/AO.58.004099.

[14] A. Udupa, X. Yu, L. Edwards, and L. L. Goddard, "Selective area formation of arsenic oxide-rich octahedral microcrystals during photochemical etching of n-type GaAs," *Optical Materials Express*, vol. 8, no. 2, pp. 289–294, 2018, doi: 10.1364/OME.8.000289.

[15] B. K. Tsai, C. C. Cooksey, D. W. Allen, C. C. White, E. Byrd, and D. Jacobs, "Exposure study on UV-induced degradation of PTFE and ceramic optical diffusers," *Applied Optics*, vol. 58, no. 5, pp. 1215–1222, 2019, doi: 10.1364/AO.58.001215.

[16] S. Uprety, A. J. Zele, B. Feigl, D. Cao, and P. Adhikari, "Optimizing methods to isolate melanopsin-directed responses," *Journal of the Optical Society of America A*, vol. 38, no. 7, pp. 1051–1064, 2021, doi: 10.1364/JOSAA.423343.

[17] M. Lei, J. Qian, X. Zhou, S. Dang, D. Dan, and Z. Wang, "Large-scale volumetric imaging of insects with natural color," in *Frontiers in Optics / Laser Science*, 2018, p. 115. doi: 10.1364/FIO.2018.JW3A.115.

[18] J. Li *et al.*, "Double optical gating for generating high flux isolated attosecond pulses in the soft X-ray regime," *Optics Express*, vol. 27, no. 21, pp. 1–8, 2019, doi: 10.1364/OE.27.030280.

[19] M. Lecca, "Generalized equation for real-world image enhancement by Milano Retinex family," *Journal of the Optical Society of America A*, vol. 37, no. 5, pp. 849–858, 2020, doi: 10.1364/JOSAA.384197.

[20] J. Ruschel *et al.*, "Current-induced degradation and lifetime prediction of 310 nm ultraviolet light-emitting diodes," *Photonics Research*, vol. 7, no. 7, pp. 36–40, 2019, doi: 10.1364/PRJ.7.000B36.

[21] G. Liu, W. Hou, and M. Han, "Unambiguous peak recognition for a silicon fabry–pérot interferometric temperature sensor," *Journal of Lightwave Technology*, vol. 36, no. 10, pp. 1970–1978, 2018, doi: 10.1109/JLT.2018.2797202.

[22] M. Strojnik, A. Beltran-Gonzalez, G. Garcia-Torales, B. Bravo-Medina, and S. Reighley, "Portable device to monitor skin condition with diffuse, multi-spectral illumination," in *Diffuse Optical Spectroscopy and Imaging*, 2019, p. 67. doi: 10.1117/12.2527218.

[23] T. Mercier, C. Krishnan, and M. D. B. Charlton, "On chip quantum dot based phosphor for efficient and tunable color conversion," in *CLEO Pacific Rim Conference*, 2018, p. 8. doi: 10.1364/CLEOPR.2018.W3A.8.

[24] X. Li, S. Qiang, B. Xu, X. Fu, G. Zhang, and Y. Wang, "Wavelength-multiplexed stereoscopic LC display using scanning backlight," *Applied Optics*, vol. 60, no. 8, pp. 2331–2338, 2021, doi: 10.1364/AO.417280.

[25] Tae Wook Kang *et al.*, "Enhancement of the optical properties of CsPbBr3 perovskite nanocrystals using three different solvents," *Optics Letters.*, vol. 45, no. 18, pp. 4972-4975, 2020, doi: 10.1364/OL.401058.

BIOGRAPHIES OF AUTHORS

Ha Thanh Tung received the Ph.D degree in physics from University of Science, Vietnam National University Ho Chi Minh City, Vietnam, he is working as a lecturer at the Faculty of Basic Sciences, Vinh Long University of Technology Education, Vietnam. His research interests focus on developing the patterned substrate with micro- and nano-scale to apply for physical and chemical devices such as solar cells, OLED, photoanode. He can be contacted at email: tunght@vlute.edu.vn.

Huu Phuc Dang received a Physics Ph.D degree from the University of Science, Ho Chi Minh City, in 2018. Currently, he is a lecturer at the Faculty of Fundamental Science, Industrial University of Ho Chi Minh City, Ho Chi Minh City, Vietnam. His research interests include simulation LEDs material, renewable energy. He can be contacted at email: danghuuphuc@iuh.edu.vn.

Dieu An Nguyen Thi received a master of Electrical Engineering, HCMC University of Technology and Education, VietNam. Currently, she is a lecturer at the Faculty of Electrical Engineering Technology, Industrial University of Ho Chi Minh City, Vietnam. Her research interests are theoretical physics and mathematical physics. She can be contacted at email: nguyenthidieuan@iuh.edu.vn.